

CONTENTS

(I) Survey and Review

1. Electromagnetic Properties of Ferrimagnetics and Their Applications from UHF to Millimeter Waves. Part I, II, III.
(Lax & Button) Microwave J. Vol. 3, No. 9, pp. 43—49, 1960.
No. 10, pp. 52—62, 1960. No. 11, pp. 49—56, 1960 (1)
2. Antiferromagnetic Materials for Millimeter and Submillimeter Devices.
(Heller et al) J.A.P. Vol. 32, No. 3, pp. 307S—312S, 1961 (26)

(II) Materials

3. Low Magnetic Saturation Ferrites for Microwave Applications.
(Van Uitert L. G.) J.A.P. Vol. 26, p. 1289—1290, 1955..... (32)
4. Nickel Copper Ferrites for Microwave Applications.
(Van Uitert L. G.) J.A.P. Vol. 27, No. 7, pp. 723—727, 1956 (33)
5. Magnesium-Copper-Manganese-Aluminum Ferrites for Microwave Applications.
(Van Uitert) J.A.P. Vol. 28, No. 3, pp. 320—322, 1957..... (38)
6. Ferrites Pour Isolateurs a Résonance dans la Bande des 1700/2,300 Mc/s.
(Hickin et al) L'Onde Elect. Vol. 39, No. 384, pp. 233—240, 1959..... (41)
7. Ferrite System for Application at Lower Microwave Frequencies.
(Jefferson & West) J.A.P. Vol. 32, No. 3, pp. 390S—391S, 1961 (49)
8. Microwave Properties of Nonstoichiometric Polycrystalline Yttrium Iron Garnet.
(Seiden) J.A.P. Vol. 31, No. 7, pp. 1291—1296, 1960..... (51)
9. Microwave Properties of Polycrystalline Hybrid Garnets.
(Harrison et al) J. Amer. Cer. Soc. Vol. 44, No. 5, pp. 214—220, 1961..... (57)
10. L-Band Ferromagnetic Resonance Experiments at High Peak Power Levels.
(Schlömman et al) Trans. I.R.E. MTT-8, No. 1, pp. 96—100, 1960..... (64)
11. High Power Ferromagnetic Resonance at X-Band in Polycrystalline Garnets and Ferrites.
(Green & Schlömman) Trans. I.R.E. MTT-8, No. 1, pp. 100—103, 1960..... (68)
12. Dependence of the Resonance Line-Width of Microwave Ferromagnetic Materials on Incident RF Power.
(Carter et al) Trans. I.R.E. MTT-9, No. 2, pp. 195—197, 1961 (72)
13. Ferrimagnetic Resonance of Single-Crystal Barium Ferrite in the Millimeter Wave Region.
(Franklin F. Y. Wang et al) J.A.P. Vol. 32, No. 8, pp. 1621—1622, 1961..... (75)

14. Preparation and Properties of Thin Ferrite Films.
(Banks et al) J.A.P. Vol. 32, Suppl. No. 3, pp. 44S—45S, 1961 (76)
15. Ferrites with Planar Anisotropy at Microwave Frequencies.
(Bady) Trans. I.R.E. MTT-9, No. 1, pp. 52—62, 1961 (77)
16. Ferrite Thin Films.
(Lemaire et al) J.A.P. Vol. 32, Suppl. No. 3, pp. 46S—47S, 1961 (88)

(III) Methods of the Preparation of Polycrystalline Materials

17. The Preparation of Magnesium-Manganese Ferrite for Microwave Applications
(Robinson) Proc. I.E.E. Vol. 104B, Suppl. No. 5, pp. 159—164, 174—178, 1957..... (90)
18. Method for Forming Large Ferrite Parts for Microwave Applications.
(Uitert et al) J.A.P. Vol. 27, No. 11, pp. 1385—1386, 1956 (95)
19. Preparation of Polycrystalline Ferrimagnetic Garnet Materials for Microwave Applications.
(Wolf & Rodrigue) J.A.P. Vol. 29, No. 1, pp. 105—108, 1958 (96)
20. Ferrimagnetic Resonance Line Widths and Phase Distributions in Sintered Yttrium Iron Garnets.
(Van Uitert et al) J. Amer. Cer Soc. Vol. 42, No. 10, pp. 471—473, 1959 (100)
21. Reaction Kinetics of Polycrystalline Yttrium Iron Garnet.
(Holmquist et al) J. Amer. Cer. Soc. Vol. 44, No. 4, pp. 194—196, 1961 (103)

(IV) Methods of the Growth of Single Crystals

22. The Growth of Oxide Single Crystals Containing Transition Metal Ions.
(Harrison) Research Appl. in Ind. Vol. 12, pp. 395—403, 1959..... (106)
23. The Growing of Single Crystals of Magnetite.
(Smiltens) J. Chem. Phys. Vol. 20, No. 6, pp. 990—994, 1952 (115)
24. Growth of Single Crystals of Incongruently Melting Yttrium Iron Garnet by Flame Fusion Process.
(Rudness et al) J. Amer. Cer. Soc. Vol. 43, No. 1, pp. 17—22, 1960..... (119)
25. フェライト単結晶の生長.
(坂本信彦) 金属物理, Vol. 3, No. 1, pp. 23—24, 1957..... (125)
26. The Growth of Single Crystals of Magnetic Garnets.
(Nielsen et al) J. Phys. Chem. Solids. Vol. 5, pp. 202—207, 1958 (127)
27. Improved Method for the Growth of Yttrium-Iron and Yttrium-Gallium Garnets.
(Nielsen) J.A.P. Vol. 31, Suppl. No. 5, pp. 51S—52S, 1960 (133)
28. Characteristic Imperfections in Flux-Grown Crystals of Yttrium Iron Garnet.
(Lefever et al) J. Amer. Cer. Soc. Vol. 44, No. 3, pp. 141—144, 1961..... (135)

29. Growth of Yttrium Iron Garnet Single Crystals by the Floating Zone Technique.
(Abernethy et al) J.A.P. Vol. 32, No. 3, pp. 376S—377S, 1961 (139)
30. Growth of Single Crystals of Yttrium Aluminium Garnet from Lead Oxide-Lead Fluoride Melts.
(Lefever et al) J.A.P. Vol. 32, No. 5, pp. 962—963, 1961..... (141)

(V) Applications

31. Origin and Use of Instabilities in Ferromagnetic Resonance.
(Suhl) J.A.P. Vol. 29, No. 3, pp. 416—421, 1958 (142)
32. Theory of Parametric Amplification Using Nonlinear Reactances.
(Bloom, Chang) RCA Rev. Vol. 18, No. 4, pp. 578—593, 1957..... (148)
33. Theoretical Limitations to Ferromagnetic Parametric Amplifier Performance.
(Damon & Eshbach) Trans. I.R.E. MTT-8, No. 1, pp. 4—9, 1960..... (164)
34. Experimental Study of the Modified Semistatic Ferrite Amplifier.
(Whirry & Wang) J.A.P. Vol. 30, Suppl. No. 4, pp. 150S—151S, 1959..... (170)
35. A Ferromagnetic Amplifier Using Dielectric Loading.
(Gruenberg) Proc. I.R.E. Vol. 48, pp. 1779—1780, 1960..... (172)
36. Microwave Devices—Theoretical and Experimental Characteristics of a Ferromagnetic Amplifier Using Longitudinal Pumping.
(Denton) J.A.P. Vol. 32, No. 3, pp. 300S—307S, 1961 (173)
37. Ka-Band Ferrite Amplifier.
(Roberts) Proc. I.R.E. Vol. 49, No. 6, p. 963, 1961..... (181)
38. Pulsed Millimeter-Wave Generation Using Ferrites.
(Elliott et al) Trans. I.R.E. MTT-9, No. 1, pp. 92—94, 1961 (182)
39. Microwave Power Limiters Using Ferrites.
(Soochoo) Solid State Physics in Electronics & Telecommunications. Vol. 3, Pt. 1, pp. 275—291, 1960 (185)
40. Low-Level Garnet Limiters.
(Arams et al) Proc. I.R.E. Vol. 49, No. 8, pp. 1308—1313, 1961..... (202)
41. Power Limiting in the 4-KMC to 7-KMC Frequency Range Using Lithium Ferrite.
(Rossol) Proc. I.R.E. Vol. 49, No. 10, p. 1574, 1961 (208)
42. Low-Temperature Microwave Power Limiter.
(Sansalone) Trans. I.R.E. MTT-9, No. 3, pp. 272—273, 1961 (209)
43. A Y-Junction Strip-Line Circulator.
(Milano et al) Trans. I.R.E. MTT-8, No. 3, pp. 346—351, 1960..... (211)
44. Circulators at 70 and 140 KMC.
(Thaxter et al) Proc. I.R.E. Vol. 48, No. 1, pp. 110—111, 1960 (217)
45. Stripline Y-Circulators for the 100 to 400 MC Region.
(Buehler et al) Proc. I.R.E. Vol. 49, No. 2, pp. 518—519, 1961 (218)
46. On the Theory of the Ferrite Resonance Isolator.
(Schlömann) Trans. I.R.E. MTT-8, No. 2, pp. 199—206, 1960..... (219)
47. Ferrite High-Power Effects in Waveguides.

- (Stern & Mangiaracina) Trans. I.R.E. MTT-7, pp. 11—15, 1959 (226)
48. Temperature Effects in Microwave Ferrite Devices.
(Melchor & Vartanian) Trans. I.R.E. MTT-7, pp. 15—18, 1959..... (230)
49. Ferrite Shape Considerations for UHF High-Power Isolators.
(Stern) Trans. I.R.E. MTT-8, No. 5, p. 565, 1960..... (234)
50. Operation of the Field Displacement Isolator in Rectangular Wave-Guide.
(Comstock & Fay) Trans. I.R.E. MTT-8, No. 6, pp. 605—611, 1960..... (235)
51. Millimeter-Wave Field-Displacement-Type Isolators with Short Ferrite Strips.
(Ishii et al) Proc. I.R.E. Vol. 49, No. 5, pp. 975—976, 1961 (242)
52. Magnetically-Tunable Microwave Filters Using Single-Crystal Yttrium-Iron-Garnet Resonators.
(Carter) Trans. I.R.E. MTT-9, No. 3, pp. 252—260, 1961..... (243)
53. A Ferrimagnetic Limiter-Isolator.
(Brown & Harrison) Proc. I.R.E. Vol. 49, No. 10, p. 1575, 1961..... (252)

(VI) Bibliography

54. Report of Advances in Microwave Theory and Techniques—1956.
(King) Trans. I.R.E. MTT-5, No. 2, pp. 83—86, 1957 (253)
55. Report of Advances in Microwave Theory and Techniques—1957.
(Beam) Trans. I.R.E. MTT-6, No. 3, pp. 251—263. [11]—[17], [27]—[33], [235]—[249], 1958 (257)
56. Report of Advances in Microwave Theory and Techniques in U.S.A.—1958.
(Beam & Brodwin) Trans. I.R.E. MTT-7, No. 3, pp. 308—323, Parametric Amplifier [1]—[6]; Anisotropic Waveguide [176]—[213], 1959 (270)
57. Report on Advances in Microwave Theory and Techniques—1960.
(Hansen & Weiss) Trans. I.R.E. MTT-9, No. 4, pp. 278—290, 1961..... (286)
58. Parametric Devices and Masers: An Annotated Bibliography.
(Mount & Begg) Trans. I.R.E. MTT-8, No. 2, pp. 222—225, 1960.
I. Review Articles [1]—[18]; Ferrite Type [39]—[58]..... (299)

Electromagnetic Properties of Ferrimagnetics and Their Applications from UHF to Millimeter Waves

BENJAMIN LAX and KENNETH J. BUTTON

LINCOLN LABORATORY*

MASSACHUSETTS INSTITUTE OF TECHNOLOGY

Lexington

Massachusetts

FIRST OF THREE PARTS

Developments during the past three years in both the experimental and theoretical studies of ferrimagnetic materials in waveguides have encompassed a broad range of activities. It is no longer appropriate to refer to this field as "microwave ferrites," as in the past, because nonreciprocal devices now exist which use ferrimagnetic garnet materials and antiferromagnetic materials. Furthermore, the frequency range of application is not restricted to the microwave range but extends throughout both the UHF and also the millimeter wave region. The review of some of these most recent accomplishments which follows will be concerned not only with the fundamental advances in the understanding of ferromagnetic materials, but also with the application of this knowledge which has resulted in the invention and development of new and improved devices. A large portion of this paper will also be devoted to the description of the principles of operation and the performance characteristics of a number of these UHF, microwave and millimeter wave components.

PART I

WAVE PROPAGATION IN FERRITE LOADED STRUCTURES

Rectangular Waveguide
Fundamental Waveguide Mode
Anomalous Gyromagnetic Modes
Ferrite-Guided Modes
Nonreciprocal Coaxial Structure
Tunable Cavity Resonator

PART II SPIN WAVES

Spin Wave Spectrum
Magnetostatic Modes

LINE WIDTH IN FERRIMAGNETS

Role of Spin Waves
Role of Impurities

NONLINEAR PROPERTIES OF FERRITES

Harmonic Generation
Saturation of the Spin System
Ferromagnetic Amplifier
Electromagnetic Operation
Modified Semi-static Operation
Longitudinal Pumping
Gain-Bandwidth
Microwave Power Limiter

PART III

FERRITE DEVICES IN UHF BANDS

Low-Field Magnetic Losses
Aluminum-Doped Ferrites
High-Power Devices
Three-Port Circulator

RECIPROCAL PHASE SHIFTER DEVELOPMENTS AT MILLIMETER WAVELENGTHS

High-Anisotropy Ferrites
Three-Port Circulator
Antiferromagnetic Devices

I. INTRODUCTION

Some of the advances in research covered by this review constitute important breakthroughs into undeveloped areas formerly inaccessible because of the need for fundamental exploration. Other advances have involved the more complete development of topics that have been pursued successfully for several years. A major item of the latter category has been the theoretical problem of wave propagation in waveguides containing ferrites. The anomalous gyromagnetic modes in rectangular guide and non-reciprocal propagation in simulated coaxial line have received recent attention. A new problem that has now been managed successfully is the solution for the tunable resonant modes of ferrite loaded cavities.

* Operated with support from the U.S. Army, Navy, and Air Force.

From a fundamental viewpoint, our knowledge of spin waves and their importance in ferromagnetic resonance phenomena has been clearly established with the use of a simultaneous theoretical and experimental approach. Their contribution to the ferrite resonance loss mechanism has been identified. Some of this has been possible only through the discovery and subsequent experimentation with the new garnet materials which have permitted a more detailed examination of the nature of magnetic losses at microwave frequencies. There is now a clearer understanding of the nonlinear behavior of ferrites and garnets under conditions of high signal power. This has led to the development of high-power isolators and to the invention of entirely new devices such as the ferromagnetic amplifier, the harmonic generators and the microwave power limiter.

A genuine breakthrough has occurred in applications with the invention of millimeter devices such as isolators and circulators at wavelengths as short as two millimeters. High frequency isolators which require unusually large dc magnetic biasing fields have, until recently, utilized the high-anisotropy uniaxial magnetic oxides having large internal fields. Today, however, the use of antiferromagnetic materials having internal fields from fifty to hundreds of kilogauss permit nonreciprocal devices to be operated from the millimeter well into the far infrared range.

The conventional isolators and circulators have been extended to operate in the UHF region in both rectangular guide and coaxial line through the use of garnets and aluminum-substituted ferrites. The invention of the ferrite Y-circulator has provided a compact device which has

demonstrated its usefulness in both the UHF and millimeter wave region. Finally, much higher performance is now available in fast, electronically-controlled microwave switches and reciprocal ferrite phase shifters for antenna scanning applications.

II. WAVE PROPAGATION IN FERRITE-LOADED STRUCTURES

The earliest theoretical treatments of propagation in ferrite-loaded transmission lines dealt with the set of modes propagating in cylindrical waveguide containing an axially-magnetized ferrite rod¹ and also the fundamental TE mode in rectangular waveguide containing a ferrite magnetized transversely to the direction of propagation. Although the electromagnetic theory for the cylindrical waveguide developed a more complete set of modes, the solution for rectangular waveguide² proved to be more amenable to numerical evaluation.³ This theory has recently led to the discovery of a new class of modes indigenous to ferrite-loaded waveguide and has also provided a physical interpretation in terms of their unique field patterns. It is now possible to classify three varieties of propagating modes that can exist in a rectangular waveguide containing a transversely-magnetized ferrite slab. The first category contains the fundamental mode which may be distorted by the ferrite slab in such a way as to introduce nonreciprocal propagation. These may be called the *waveguide modes*. The second class are unidirectional modes. Since each of these propagates only in one direction, they have no analog in empty waveguide or in a guide containing an isotropic medium. They arise as a consequence of the tensor properties of the gyromagnetic medium. The lowest mode of this class is a TE mode and has been called the "ferrite-dielectric" mode. The higher modes of this *anomalous gyromagnetic class* are not purely TE nor TM but have additional cartesian components of the microwave electric and magnetic field. The final class of modes are also neither TE nor TM but they are not unidirectional. They propagate in both the forward and reverse directions and the propagation constant is nonreciprocal. Unlike the distorted waveguide modes, the electromagnetic energy is contained largely within the ferrite slab and their existence depends upon the slab thickness. Therefore, we shall designate these as *ferrite-guided modes*.

Nonreciprocal propagation in coaxial transmission line has also been described by theoretical consideration of the TE mode distorted by dielectric loading. The boundary value solution of the simulated loaded coaxial line has

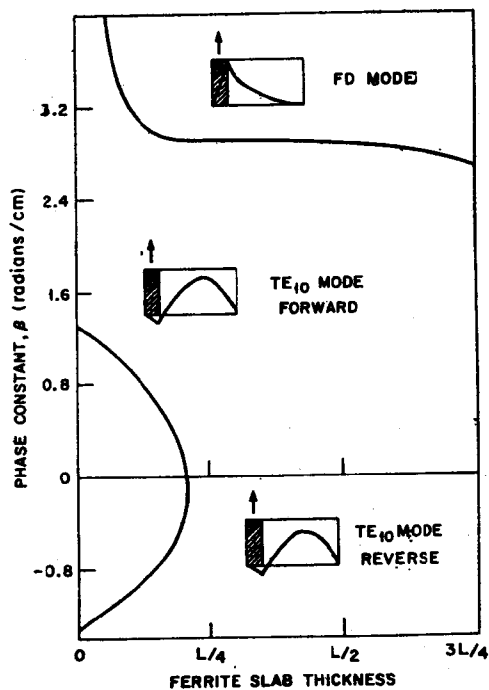


Figure 1 — Phase constant vs slab thickness for a transversely magnetized ferrite slab against the side wall of a rectangular waveguide under conditions of negative effective permeability. Solutions (neglecting losses) are shown for the nonreciprocal TE₁₀ mode and the ferrite-dielectric mode which is the lowest mode of the anomalous gyromagnetic class. A frequency of 9000 mc was used for standard X-band waveguide of width L. (After Lax and Button).

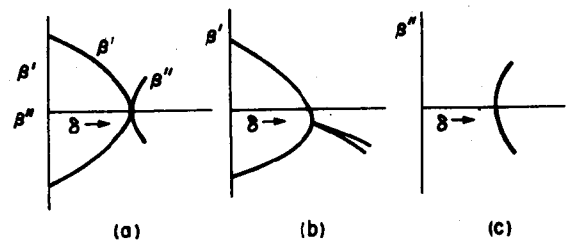


Figure 2 — The propagation constant vs slab thickness δ for the TE₁₀ mode under conditions shown in Figure 1 for (a) ordinary waveguide cutoff; (b) and (c) ferrite-loaded guide. Although losses are neglected, a complex propagation constant $\beta' + j\beta''$ is obtained indicating an evanescent mode beyond "cut-off". (After C. T. Tai).

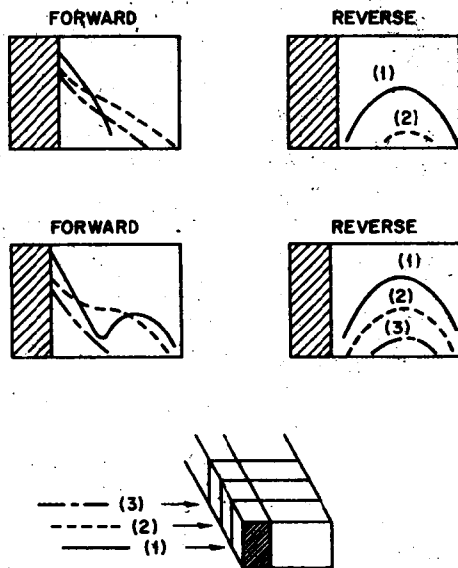


Figure 3 — Experimental determination of the relative rf electric field intensity in a ferrite loaded waveguide for two slab thicknesses, showing the evanescent waveguide mode propagating in the reverse direction and the ferrite dielectric mode in the forward direction. The thicker slab (top) quenches the waveguide mode more effectively. (After Angelakos).

provided the field patterns, and the nonreciprocal phase shift has been calculated for both the UHF and microwave regions.

Rectangular Waveguide

The technique of solving propagating mode problems in rectangular waveguide involves the substitution of an assumed field pattern into Maxwell's equations and the subsequent matching of boundary conditions at the walls of the guide and at the ferrite-air interface. Since the solution takes the form of a transcendental equation and the computations are usually complicated, the problem is often solved for one class of modes at a time.

Fundamental Waveguide Mode—The phase constants for forward and reverse propagation in the nonreciprocal waveguide mode are shown at the lower left of Figure 1. As the slab thickness is increased, the phase constants for both directions approach zero and the calculated electric field pattern shown in the inset appears to be crowded into an effectively smaller guide. At a critical thickness, the phase constants go to zero and the mode is cut off. However, the theoretical solutions for the TE_{10} mode have been extended into the "cut-off" region by C. T. Tai,⁸ and he has shown that the propagation constant becomes complex proving that the waveguide mode is not actually cut off in the usual sense but becomes evanescent. Whereas, in the absence of ferrite (Figure 2a), the solution becomes purely imaginary at cut-off, the solutions for a ferrite slab in a waveguide (Figures 2b and c) have a real and imaginary part.

The experimental consequences^{6,7} of this behavior are shown in Figure 3. The relative rf electric field intensity has been mapped through the use of a small transverse E-probe inserted in the top of the guide at points in the three planes shown. The waveguide mode (reverse propa-

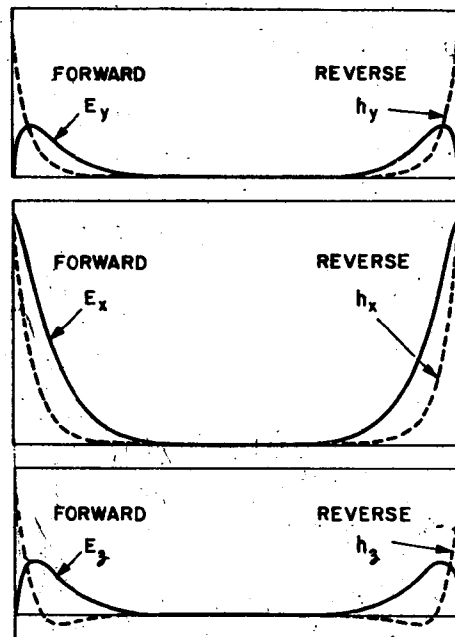


Figure 4 — The field patterns for a ferrite-metal mode in waveguide completely filled with ferrite. The field intensities are for forward propagation and at the other side for reverse propagation. This would be a uni-directional mode if the ferrite were in contact with only one wall. (After Barzilai and Gerosa).

gation) is evanescent and the penetration is shallower for the thicker slab. Forward propagation takes place in the "ferrite-dielectric" mode which is the unidirectional solution at the top of Figure 1.

Anomalous Gyromagnetic Modes—The higher modes of this class will propagate even in arbitrarily small completely-filled waveguide when the effective permeability of the ferrite is negative. The problem of propagation in a rectangular guide completely filled with ferrite was formulated by Mikaelyan⁹ and in the parallel-plate analog by Van Trier.⁹ The general form of these solutions took into account the birefringent character of the ferrite and did not restrict the solutions to simple TE or TM mode patterns. Seidel¹⁰ has recently applied this type of formulation to the guide containing a slab against the wall and given the physical and analytical interpretation of anomalous unidirectional mode propagation. These modes have now been classified by Seidel and Fletcher.¹¹ They simplified the problem considerably by confining their attention to arbitrarily small guide, in which only higher unidirectional modes propagate, all others being cut off. Thompson¹² had previously demonstrated the existence of this phenomenon experimentally. Seidel found solutions where the electric field reached a maximum within the ferrite near the metal wall of the guide. A linear combination of such birefringent rays permitted the boundary condition at the metal wall to be satisfied. Then, using the small-guide restriction, the following explicit expression for the phase constant, β , was obtained for the "ferrite-metal" (FM) modes:

$$\beta = \frac{1}{\kappa} \frac{m\pi}{d} \left(\frac{\mu\kappa^2}{\kappa^2 - \mu^2} \right)^{1/2} \quad \text{FM modes}$$

where μ and κ are the diagonal and off-diagonal components of the ferrite permeability tensor. The distance d denotes the waveguide height, and the order m of the mode is defined as the number of half cycles of sinusoidal variation along the direction of the transverse dc magnetic field; $m=0$ are the TE modes which are not admitted by the small-guide restriction. Figure 4 shows a plot made by Barzilai and Gerosa¹³ of field patterns for a mode of this sort for the guide completely filled with ferrite. If some of the ferrite were removed from contact with either the right or left wall, this mode would propagate only in one direction. A plot of the phase constant for several FM modes for half-filled guide is shown in the upper part of Figure 5. The FA (ferrite-air) modes shown are those which have the peaks of their field patterns at the interface between ferrite and air in the half-filled guide. Again, Seidel and Fletcher discovered these by satisfying the boundary conditions with linear combinations of only those solutions which have a peak intensity near the interface. These restrictions resulted in the following remarkably simple expressions for the phase constant for each type of "ferrite-air" mode:

$$\beta = -\frac{1}{\kappa} \frac{m\pi}{d} \left(\frac{\mu\kappa^2}{\kappa^2 - \mu^2} \right)^{1/2} \quad \text{FA I}$$

$$-\kappa\beta = \left[\left(\frac{m\pi}{d} \right)^2 + \beta^2 \right]^{1/2} + \mu \left[\frac{1}{\mu} \left(\frac{m\pi}{d} \right)^2 + \beta^2 \right]^{1/2} \quad \text{FA II}$$

It should be noted that the FM mode propagates in one direction while propagation in the other direction takes place via the FA I mode.

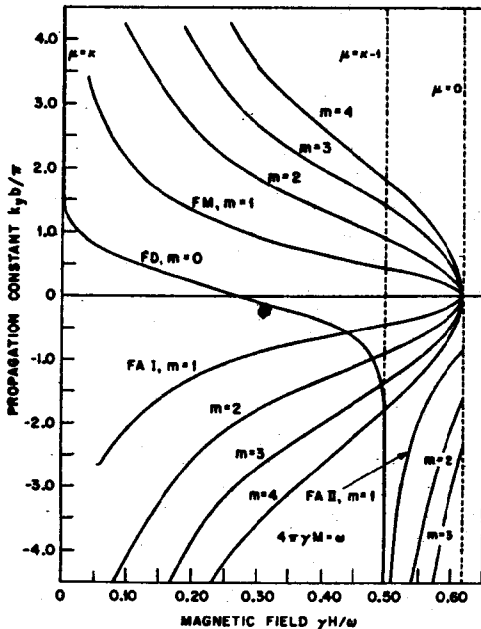


Figure 5 — Typical anomalous gyromagnetic mode spectrum in half-filled small guide as a function of magnetic field. (After Seidel and Fletcher).

Ferrite-Guided Modes—Figure 6 shows the phase constant νs ferrite slab thickness obtained from the general solution carried out by Barzilai and Gerosa.¹⁴ As the slab (against the left wall) is made thicker, the ferrite guided modes begin to appear and, at the slab thickness designated by the two black dots, the field patterns in this mode have the form shown in Figure 7. The microwave energy is concentrated largely within the ferrite. This is neither a TE nor TM mode because all components of both the electric and magnetic fields exist. These modes do not depend upon the guide width but on the slab width and unlike the unidirectional modes which propagate in arbitrarily small guide, these can be cut off by making the slab (or the guide) sufficiently small.

Nonreciprocal Coaxial Structure

The TEM mode of coaxial transmission line is unsuitable for nonreciprocal ferrite devices unless the mode can be distorted sufficiently to create a rotating rf magnetic field vector. Since this has been accomplished recently, coaxial circulators and ferrite resonance isolators are available in the UHF bands which have the compact, broadband (and low power) characteristics of coaxial line. It was shown by Seidel¹⁵ that it is possible to develop a nonreciprocal structure in coaxial line by distorting the azimuthal symmetry of the TEM mode with adielectric and thereby generate a longitudinal component of the rf magnetic field. The two magnetic components form a

vector which rotates as the wave pattern moves along the line. When a transversely-magnetized ferrite is placed in this region of the rotating rf magnetic field, nonrecipro-

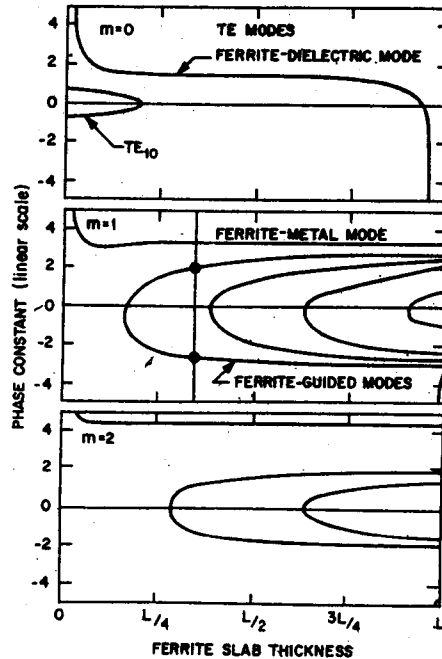


Figure 6 — Phase constant as a function of ferrite slab thickness showing the three classes of modes propagating in ferrite loaded rectangular waveguide. The solutions were obtained for a frequency of 9000 mc, for standard X-band waveguide of width L . (After Barzilai and Gerosa).

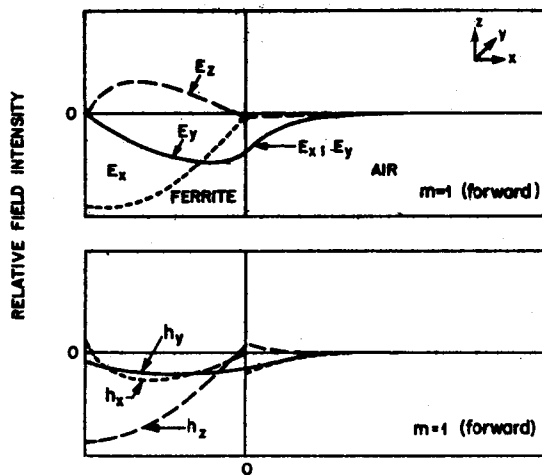


Figure 7 — Microwave field patterns of a ferrite-guided mode for forward propagation only under the conditions denoted by the two black dots in the previous figure. (After Barzilai and Gerosa).

cal be experienced. Nonreciprocal attenuation has been demonstrated experimentally by Duncan, Swern, Tomiyasu and Hannwacker.¹⁶ The analytical problem for the reciprocal coaxial phase shifter containing a small ferrite only was formulated by Sucher and Carlin¹⁷ by making use of the parallel plate analog of the coaxial line. They obtained a small nonreciprocal effect because the ferrite itself has a relatively large dielectric constant which distorts the TEM mode. When a material of relatively large dielectric constant K_e is enclosed by the ferrites as shown in Figure 8 the field distortion is greatly enhanced. Numerical solutions of the boundary value problem in the simulated coaxial line shown in the lower part of Figure 8 were carried out by Button¹⁸ who obtained differential phase shifts as large as one radian per centimeter of line length at 2000 mc as shown in Figure 9. The differential phase shift is small if the TEM mode is only slightly distorted by either a small amount of dielectric or a small dielectric con-

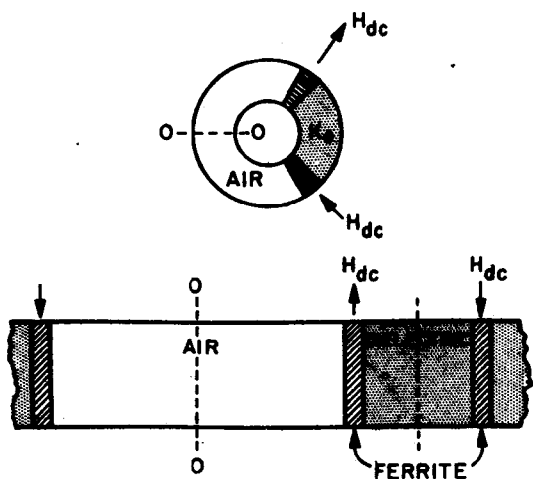


Figure 8 — The cross-section of the ferrite nonreciprocal coaxial phase shifter (upper figure) showing the dielectric loading, K_e , and two transversely magnetized ferrite slabs. The infinite parallel plate analog is constructed by slitting the line at O-O and unrolling it (After Button).

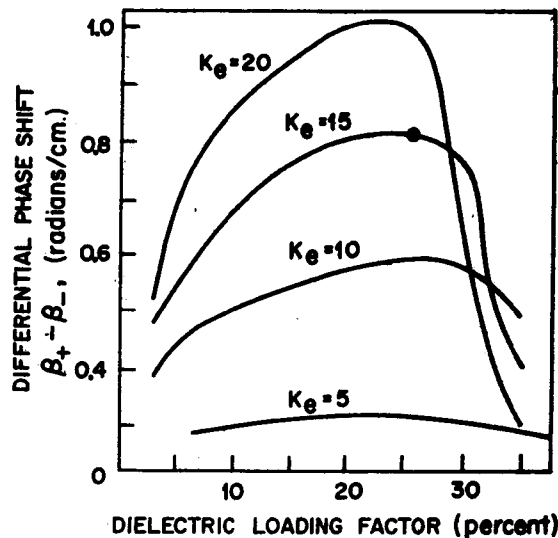


Figure 9 — Theoretical differential phase shift vs amount of dielectric at a frequency of 2000 mc for a 1 5/8 inch diameter coaxial line. Smaller amounts of dielectric must be used for large K_e to avoid the dielectric-waveguide effect. (After Button).

stant. The effect also drops off precipitously if the amount of dielectric is too large because nearly all of the microwave energy is concentrated within the dielectric with little remaining in the region where the ferrites are located. Of course, larger amounts may be used at longer wavelengths. The results of the boundary value solution have been used to plot the field patterns within the loaded line as shown in Figure 10. The peak of the electric intensity occurring within the dielectric creates a gradient in the transverse electric field which does not exist in the

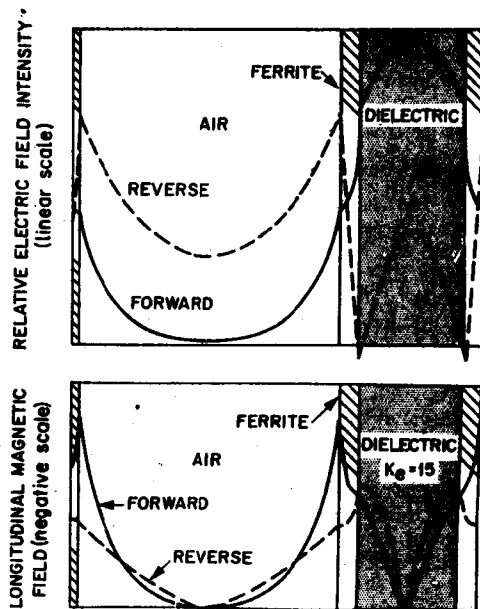


Figure 10 — The transverse rf electric field intensity (upper figure) for the nonreciprocal coaxial phase shifter. The longitudinal component of the rf magnetic field, which does not exist in empty coaxial line, combines with the transverse magnetic component (not shown) to provide the rotating magnetic vector needed for nonreciprocal effects. (After Button).

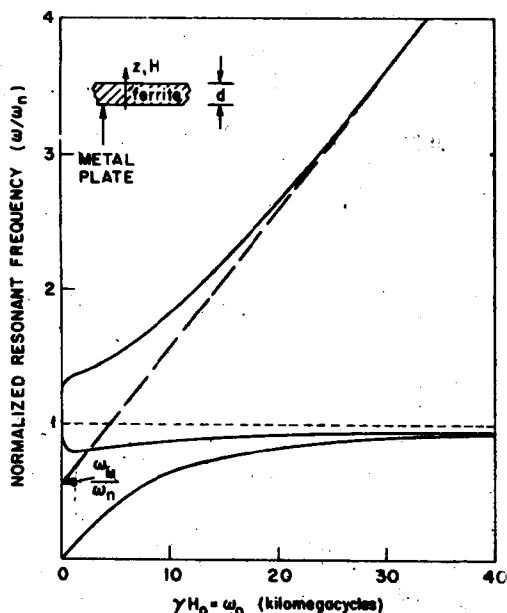


Figure 11 — The resonant frequencies (normalized by the zero-field resonance) for the completely-filled infinite parallel-plate cavity shown in the inset. The frequencies have been plotted as a function of dc magnetic field intensity for the magnetic field perpendicular to the plates from the cubic equation of Equation 3.

undistorted TEM mode. This gives rise to a large longitudinal magnetic component near the interface which is needed for the ferrite to exhibit nonreciprocal properties.

This numerical solution has been extended to the UHF region by Boyet, Weisbaum and Gerst¹⁹ who have made calculations of the nonreciprocal phase shift in coaxial line loaded with ferrite and dielectric and have found that a circulator can be constructed at 400 mc which would be only five inches long. They have also shown that the external dc magnetic field can be adjusted to achieve broad-band characteristics.

The Tunable Cavity Resonator

The resonator frequency of a cavity containing a ferrite can be tuned by varying the external dc magnetic field applied to the ferrite. If the cavity is to contain more than about one percent ferrite by volume, the resonant frequencies of the cavity modes will vary over a wide range as a function of external field and the mode patterns will be distorted substantially. The essential features of the cavity problem, including the resonant frequencies, can be obtained from the simplest possible case shown in the insert of Figure 11 or Figure 12. This is an infinite slab of ferrite bounded by two infinite metal plates. Since the component of the electric field parallel to the plates must vanish at the conducting surfaces, we must have a field of the form $\vec{E} = E_z \sin k_z z$ where $k_z = n\pi/d$. The familiar form of the dispersion relation from Maxwell's equations reduces to

$$k_z^2 = \frac{\omega^2}{c^2} K_e \mu_{\text{eff}} \text{ where } \mu_{\text{eff}} \text{ is the dimensionless}$$

"effective permeability" of the ferrite composed of the elements of the permeability tensor. Thus the solution of the problem is given by

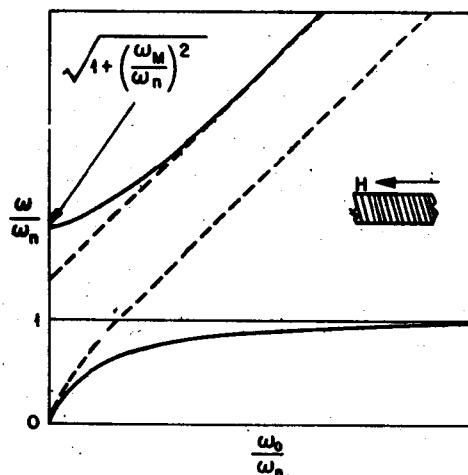


Figure 12 — The normalized resonant frequencies as a function of applied field for the dc magnetic field parallel to the metal walls of the completely-filled infinite parallel-plate cavity shown in the inset. These are the two roots of the biquadratic of Equation 4. (After Heller).

$$k_z^2 = \frac{\omega^2}{c^2} K_e \mu_{\text{eff}} = (n\pi/d)^2 = \frac{\omega_n^2}{c^2} K_e \quad (1)$$

or

$$\omega^2 \mu_{\text{eff}} = \omega_n^2$$

where ω_n is the resonant frequency of the cavity at zero field where the medium within the cavity is unmagnetized and is then characterized only by its dielectric constant, K_e . For the case shown in Figure 11 where the external field is perpendicular to the plates, $\mu_{\text{eff}} = \mu_{\pm} = 1 + [\omega_M/(\omega_0 \mp \omega)]$ and Equation (2) becomes

$$\omega^2 \left[1 + \frac{\omega_M}{\omega_0 \mp \omega} \right] = \omega_n^2 \quad (3)$$

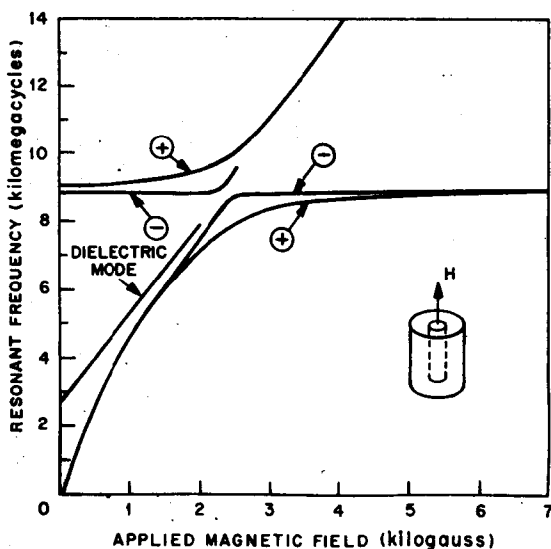


Figure 13 — The exact solutions for the TM_{110} mode in a cylindrical cavity containing a thin axial ferrite rod with a ratio of rod to cavity diameter of 0.1. The positive and negative rotating mode solutions and the ferrite-dielectric mode (extreme left) are shown (After Heller).

where ω_M and ω_0 are proportional to the ferrite magnetization and the applied field, respectively, and ω is the resonant frequency of the cavity in the presence of a field. The three modes of resonance (as a function of applied field) which are solutions of this cubic equation are shown in Figure 11.

If the same parallel-plate cavity has the external field applied parallel to the plates as shown in Figure 12, it is only necessary to substitute into Equation (2) the effective permeability for a ferrite magnetized transverse to the direction of propagation which yields a biquadratic equation in ω :

$$\omega^4 - \omega^2 [(\omega_0 + \omega_M)^2 + \omega_n^2] + \omega_n^2 (\omega_0^2 + \omega_M \omega_0) = 0 \quad (4)$$

A plot of the two roots of this equation as a function of dc magnetic field intensity is shown²⁰ in Figure 12.

The latter parallel-plate analogy applies directly to the problem of the TM modes of both the completely-filled rectangular cavity²¹ and the completely-filled cylindrical cavity where ω_n , in each case, represents the appropriate zero-field solution for the particular geometry. For example $\omega_n^2 \rightarrow \omega_{n,m}^2 \propto (l\pi/a)^2 + (m\pi/b)^2$ for the rec-

tangular cavity. Heller²⁰ has pointed out that the TM_{lmo} modes of the cylindrical resonator containing an axially-magnetized ferrite rod have a relatively simple solution because these are the modes with field components independent of the height of the cylinder. Thus, with the axial dc field parallel to the cylindrical walls the resonant frequencies should be similar to Figure 12. Heller's results for the TM_{110} mode of the cylindrical cavity containing a longitudinally magnetized thin axial rod of ferrite are shown in Figure 13. Here the solutions split for each sense of rotation of the mode when l is not equal to zero. Heller has also plotted field patterns,²⁰ worked out results for higher TM_{lmo} modes and observed satisfactory agree-

ment with experiments for the TM_{010} mode. The one distinction between the partially-filled and completely-filled cavity is the existence of the ferrite-dielectric mode shown in Figure 13, which is analogous to that found in waveguide.

NEXT MONTH — Spin Waves, Line Width in Ferrimagnetics, Nonlinear Properties of Ferrites.

References

1. H. Suhl and L. R. Walker, "Faraday Rotation of Guided Waves," *Phys. Rev.*, Vol. 86, pp. 122-123; Jan. 1952.
2. "Topics in Guided-Wave Propagation Through Gyromagnetic Media: The Completely Filled Cylindrical Guide," *Bell System Tech. J.*, Vol. 33, pp. 579-659; Jan. 1954.
3. H. Gamo, "The Faraday Rotation of Waves in Circular Waveguide," *Jour. Phys. Soc. Japan*, Vol. 8, pp. 176-182; March 1953.
4. M. L. Kales, "Modes in Waveguides that Contain Ferrites," *J. Appl. Phys.*, Vol. 24, pp. 604-608; May 1953.
5. A. A. T. M. Van Trier, "Guided Electromagnetic Waves in Anisotropic Media," *Appl. Sci. Res.*, Vol. B3, p. 305; 1953.
6. M. L. Kales, H. N. Chait and N. G. Sakiotis, "A Nonreciprocal Microwave Component," *J. Appl. Phys.*, Vol. 24, pp. 816-817; June 1953.
7. B. Lax, K. J. Button and L. M. Roth, "Ferrite Phase Shifters in Rectangular Waveguide," *J. Appl. Phys.*, Vol. 25, pp. 1414-1421; Nov. 1954.
8. B. Lax and K. J. Button, "Theory of New Ferrite Modes in Rectangular Waveguide," *J. Appl. Phys.*, Vol. 26, pp. 1184-1185; Sept. 1955; "New Ferrite Mode Configurations and Their Applications," *J. Appl. Phys.*, Vol. 26, pp. 1186-1187; Sept. 1955.
9. K. J. Button and B. Lax, "Theory of Ferrites in Rectangular Waveguides," *Transactions I.R.E.*, Vol. AP-4, pp. 531-537; July 1956.
10. Chen To Tai, "Evanescent Modes in a Partially Filled Gyromagnetic Rectangular Wave Guide," *J. Appl. Phys.*, Vol. 31, pp. 220-221; Jan. 1960.
11. T. M. Straus and G. S. Heller, "Ferrite Dielectric Mode — Experimental," Quarterly Progress Report on Solid State Research, MIT, Lincoln Laboratory, Lexington, Massachusetts, p. 50; February, 1956.
12. D. J. Angelakos, "Transverse Electric Field Distributions in Ferrite Loaded Waveguides," *IRE Transactions on Microwave Theory and Techniques*, Vol. MTT-7, pp. 390-391; July, 1959.
13. A. L. Mikaelyan, "Electromagnetic Waves in a Rectangular Waveguide Filled with Magnetized Ferrite," *Doklady, Akad. Nauk, USSR*, Vol. 98, pp. 991-994; 1954.
14. A. A. Th. M. Van Trier, "Guided Electromagnetic Waves in Anisotropic Media," *Appl. Sci. Res.*, Vol. B3, p. 305; 1953.
15. H. Seidel, "Anomalous Propagation in Ferrite-Loaded Wave Guide," *Proc. IRE*, Vol. 44, pp. 1410-1414; Oct. 1956.
16. "Gyromagnetic Modes in Waveguide Partially Loaded with Ferrite," *Bell System Tech. J.*, Vol. 38, pp. 1427-1456; Nov. 1959.
17. H. Seidel and R. C. Fletcher, "Gyromagnetic Modes in Waveguide Partially Loaded with Ferrite," *Bell System Tech. J.*, Vol. 38, pp. 1427-1456; Nov. 1959.
18. G. H. B. Thompson, "Unusual Waveguide Characteristics Associated with the Apparent Negative Permeability Obtainable in Ferrites," *Nature*, Vol. 175, pp. 1135-1137; June 1955.
19. G. Barzilai and G. Gerosa, "Modes in Rectangular Guides with Magnetized Ferrites," *Il Nuovo Cimento*, Vol. 7, pp. 685-697; March 1958.
20. G. Barzilai and G. Gerosa, "Modes in Rectangular Guides Partially Filled With Transversely Magnetized Ferrite," *Trans. I.R.E.*, Vol. AP-7, pp. S471-S474; Dec. 1959.
21. H. Seidel, "Ferrite Slabs in Transverse Electric Mode Waveguide," *J. Appl. Phys.*, Vol. 28, pp. 218-226; Feb. 1957.
22. B. J. Duncan, L. Swern, K. Tomiyasu and J. Hannwacker, "Design Considerations for Broad Band Ferrite Coaxial Line Isolator," *Proc. I.R.E.*, Vol. 45, pp. 483-490; April 1957.
23. M. Sucher and H. J. Carlin, "Coaxial Line Nonreciprocal Phase Shifter," *J. Appl. Phys.*, Vol. 28, pp. 921-922; Aug. 1957.
24. K. J. Button, "Theory of Nonreciprocal Ferrite Phase Shifters in Dielectric Loaded Coaxial Line," *J. Appl. Phys.*, Vol. 29, pp. 998-1000; June, 1958.
25. H. Boyet, S. Weisbaum, and I. Gerst, "Design Calculations for UHF Ferrite Circulators," *Trans. IRE*, Vol. MTT-7, pp. 475-476; July 1959.
26. G. S. Heller, "Ferrite Loaded Cavity Resonators," *L'Onde Electrique*, Vol. 38, special supplement no. 376, Vol. 2, pp. 588-593; Aug. 1958.
27. G. S. Heller and M. M. Campbell, "The Completely-Filled Rectangular Resonator," *Lincoln Laboratory Quarterly Progress Report on Solid State Research, M.I.T., Cambridge, Mass.*, August, 1955.

Electromagnetic Properties of Ferrimagnetics and Their Applications from UHF to Millimeter Waves

BENJAMIN LAX and KENNETH J. BUTTON

LINCOLN LABORATORY*

MASSACHUSETTS INSTITUTE OF TECHNOLOGY

Lexington • Massachusetts

SECOND OF THREE PARTS

III. SPIN WAVES

The importance of spin waves in ferrites and ferromagnetic materials has emerged from a theoretical concept and, during recent years, the subject has become of great practical interest. The particular significance to ferrite applications was recognized in connection with the high-power problem. Direct experimental verification of the spin waves was most dramatically demonstrated in spin-wave resonance experiments²³ at microwave frequencies in thin films of permalloy. Perhaps it is appropriate to introduce this topic by discussing this particular experiment and the theory of spin-wave resonance.

Spin Wave Spectrum.

The equation of motion for a classical spin wave²³ can be written in the form:

$$\frac{d\vec{M}}{dt} = \gamma (\vec{M} \times \vec{H}) + \gamma H_{ex} a^2 \frac{\vec{M} \times \nabla^2 \vec{M}}{|\vec{M}|} \quad (5)$$

where \vec{M} and \vec{H} are the total magnetization and magnetic field including the rf components. The exchange contribution has been accounted for by introducing a restoring term proportional to $\nabla^2 \vec{M}$, where H_{ex} is the equivalent internal exchange field tending to align neighboring spins and a is the lattice constant. If Equation 5 is solved for the case where the direction of propagation of the spin wave is along the direction of the applied static magnetic field, then the frequency of the spin wave is given by

$$\omega_k = \omega_0 + \omega_{ex} a^2 k^2 \quad (6)$$

where $\omega_0 = \gamma H_0$ and $\omega_{ex} = \gamma H_{ex}$ and the frequency of each of the spin waves in the series depends on its wave number, k . In a sample of thickness δ , which may be several thousand angstrom units in a thin metal film, one can specify²⁴ the wave vector in terms of the sample dimension as

$$k = n\pi/\delta \quad (7)$$

since the spin waves meet a discontinuity at the surface and can be assumed to be "pinned" at the boundary. This result is significant in that the usual ferromagnetic resonance (the uniform precessional mode for which $n=0$) is supplemented by additional resonances of higher wave number with a separation between neighboring peaks of

$$\Delta\omega = \omega_{n+1} - \omega_n = \omega_{ex} \left(\frac{\pi a}{\delta} \right)^2 \quad (8)$$

The exchange field for a metal is of the order of 10^7 gauss corresponding to an exchange frequency $\omega_{ex} \approx 10^{14}$ cps. Consequently for a film thickness of several thousand angstrom units, $\Delta\omega \approx 10^8$ cps. Thus the spacing of the spin wave peaks should be of the order of 100 oersteds. Seavey and Tannenwald²⁵ have shown that these are resolvable, have observed the spin wave spectrum up to $n=17$ and have measured the internal exchange field for permalloy.**

The expression for the spin-wave frequency for a ferrite (ellipsoid of revolution magnetized along the axis of rotation) having millimeter dimensions or larger takes on a somewhat more complicated form

* Operated with support from the U.S. Army, Navy, and Air Force.

** A thorough description of spin wave concepts has been given by P. E. Tannenwald, "Spin Waves," *the microwave journal*, Vol. 2, pp. 25-28; July, 1959.

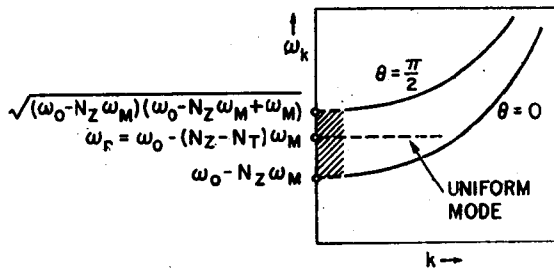


Figure 14—A plot of the spin wave spectrum from Equation 9 showing the degeneracy of the usual ferromagnetic resonance frequency (dashed line) with spin wave modes of different k and different directions of propagation. The shaded portion is the region of magnetostatic modes for $k \leq 2\pi/0.1d$ where d is the diameter of the specimen. The

expressions on the axis were obtained from Equation 9 for $k=0$ and θ as specified. The demagnetizing factors, N_x and N_T , parallel and transverse to the direction of the dc magnetic field adjust the expressions for specimens of different shape. (After H. Suhl).

$$\omega_k = [(\omega_0 - N_x \omega_M + \omega_{ex} a^2 k^2)(\omega_0 - N_x \omega_M + \omega_{ex} a^2 k^2 + \omega_M \sin^2 \theta)]^{1/2} \quad (9)$$

where $\omega_M = \gamma(4\pi M)$, N_x is the demagnetizing factor in the direction of the dc magnetic field ($N_x + N_T + N_z = 1$) and θ is the angle between the field and the direction of propagation of the spin wave. This expression is valid for short wavelength (large k) compared to the sample dimension. Figure 14 shows a plot²⁵ from Equation 9 of the spin wave frequency as a function of wave number, k . The boundaries are curves for $\theta=0$ and $\theta=\pi/2$ corresponding to z -directed and transversely directed spin waves respectively. The curves turn upward for larger values of k when the term $\omega_{ex} a^2 k^2$ becomes comparable in magnitude to the other terms of Equation 9. The horizontal line on the figure corresponds to the usual ferromagnetic resonance frequency (of an ellipsoid magnetized in the z -direction) which can be seen to be degenerate with a large number of spin waves of different wave length and different directions of propagation. Hence, any mechanism which couples energy between the uniform precessional mode and the spin waves²⁶ introduces losses and broadens the resonance line. These mechanisms will be discussed presently.

Magnetostatic Modes.

In the spectrum of spin waves which exist in specimens having finite boundaries, the uniform precessional mode represents the zero-order spin wave. The expression for the resonant frequency of this mode including the consequences of the boundary-value treatment was developed by Kittel.²⁷ Other modes of small wave number and different symmetries can also be excited in samples of finite dimension which correspond to the shaded region of Figure 14. Unlike the short-wavelength spin waves which can be represented by a sum of plane waves, the analysis of the longer wavelength magnetostatic modes must include the surface demagnetizing effects. The boundary value problem in this case is rather involved. However, it can be approximated by treating the rf magnetic fields as one does in a magnetostatic boundary value problem just as in Kittel's case. An extensive treatment has been carried out by Walker²⁸ and these magnetostatic modes have been

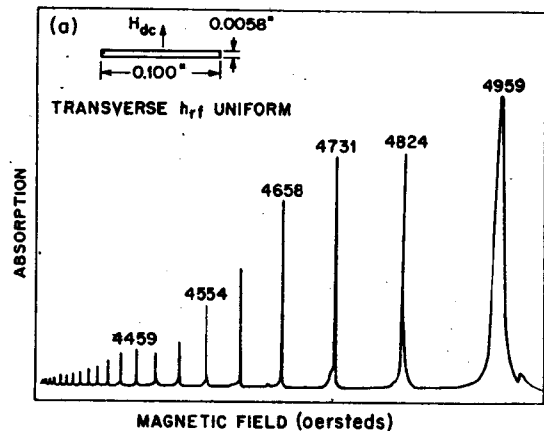


Figure 15—Magnetostatic modes at 9222 mc in a thin disk of yttrium-iron garnet magnetized perpendicular to the plane with the uniform rf driving field applied in the plane of the disk. (After Dillon).

called "Walker modes." They have been observed experimentally by White, Solt and Mercereau²⁹ and by Dillon³⁰. These modes differ physically from the uniform precessional mode³¹ in that the specimen may be placed in the microwave cavity at a nodal point of the rf magnetic field so that nonuniform precession can be excited. The wavelengths of the modes are larger than the sample dimension. However, a nodal point of the modes occurs inside the ferrite and the rf magnetization in one portion of the sample is out of phase with that of the adjacent segment. Clearly, a large number and variety of such modes can be excited. The higher the order of the mode the farther away is the frequency from that of the uniform mode. The intensity is also smaller as shown in Figure 15. The essential significance of these modes is that they demonstrate the existence of spin waves of low order and, in addition, they play an important role in the design of ferromagnetic amplifiers as modes of excitation for idler or signal frequencies.

An analysis of magnetostatic modes and spin waves showing the connection between the two types was made by Damon and Eshbach³² in which they considered the somewhat-simpler boundary value problem of a semi-infinite thin slab magnetized parallel to the plane. They found that the magnetostatic mode spectrum extends over the same frequency range as that obtained by Walker for a spheroid, namely $\omega = \gamma H_1$ to $\omega = \gamma(H_1 + 2\pi M)$. This range consists of two regions distinguished by a distinctly different mode characteristic in each. The first region, from $\omega = \gamma H_1$ to $\omega = \gamma(B_1 H_1)^{1/2}$, contains modes which are spatially harmonic plane waves or standing waves in the direction transverse to the sides of the slab. The second region, from $\omega = \gamma(B_1 H_1)^{1/2}$ to $\omega = \gamma(H_1 + 2\pi M)$, contains only surface waves³³ with exponentially decaying amplitude away from the interface of the ferrite slab into the interior of the ferromagnetic medium. These two classes of magnetostatic modes merge smoothly into surface and volume spin wave modes at higher values of wave number, k . Some of the surface mode solutions correspond to the anomalous gyromagnetic modes, i.e., ferrite dielectric and ferrite-air modes

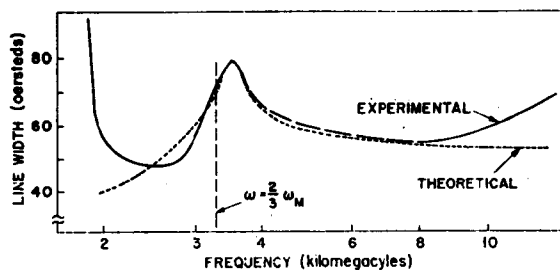


Figure 16—Resonance line width of yttrium-iron garnet sphere as a function of frequency. Domain losses in unsaturated YIG broaden the line below 2000 mc. The peak near 4000 mc indicates coupling of energy from the uniform precession to a large number of spin wave modes of the same frequency. (After Buffler).

that occur in partially-filled rectangular waveguide.^{7,10,11} The existence of these surface modes apparently has an important bearing, as we shall see, on the resonance line width problem since the line width is known to be influenced by the roughness of the surface.

IV. LINE WIDTH IN FERRIMAGNETS

It has been recognized for some time that the performance characteristics of nonreciprocal devices depends strongly on the ferromagnetic resonance line width³⁴ of the particular type of ferrite used. However, the basic physical mechanisms responsible for the breadth of the resonance line, particularly the role of spin waves in line broadening, were not understood until the behavior of ferrites was investigated under conditions of high signal power. More recently, the fundamental magnetic relaxation interactions have been described in detail through the study of ferrimagnetic garnets having resonance line widths about a hundred times smaller than ferrite lines. The contribution of impurities to the line width has also been recognized and demonstrated in garnets.

Role of Spin Waves.

Following the initial theoretical study of the nonlinear behavior of the spin system in high rf magnetic fields by Anderson and Suhl,³⁵ it was suggested by Clogston, Suhl, Walker and Anderson³⁶ that the large line width observed in ferrites (> 50 oersteds) was caused, in part, by the excitation of spin waves having frequencies ω_k the same as the mode of uniform precession, as shown in Figure 14. They showed that the frequency of a spin wave with wave number k is given by Equation 9 and suggested that energy from the uniform precessional mode can be fed into the spin wave modes which thus causes an increase in the line width. Irregularities in the magnetic lattice provide a coupling mechanism. This basic concept of the excitation of spin waves has subsequently been supported by the additional analysis of Suhl³⁵ on the nonlinear behavior at high power levels. A convincing experiment verifying the Clogston model of the spin-wave contribution to the line width has been carried out by Buffler³⁷ whose results are shown in Figure 16. He measured the line width of the uniform mode for a polycrystalline garnet sphere as a function of frequency. Above 2000 mc, $\omega_0 > \omega_M/3$, the applied magnetic field is large enough to saturate the sphere and the line width reaches a minimum because the resonant fre-

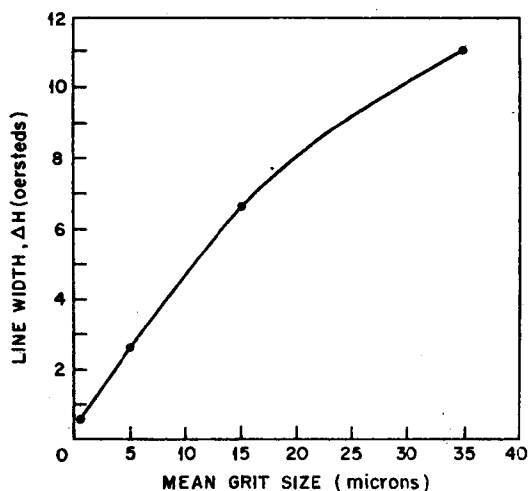


Figure 17—Line width of yttrium-iron garnet at 9300 mc vs the mean grit size of the polishing paper used to grind the spheres. (After LeCraw, Spencer and Porter).

quency, $\omega_r = \omega_0 = \gamma H_0$ is above the spin wave manifold and intersects only a small number of higher order spin waves. As the frequency is increased to $\omega_0 = 2\omega_M/3$, the resonant frequency of the uniform mode is just equal to the frequency at the top of the spin wave manifold given by the upper formula of Figure 14. Coupling to a maximum number of modes is possible and the line width goes through a maximum. At higher frequency the uniform mode approaches the bottom of the manifold where there are fewer spin wave modes and the line width again decreases.

Further insight into the nature of the interactions has emerged from the results of a number of microwave resonance experiments.³⁸ The extensive experiments of LeCraw, Spencer and co-workers³⁹⁻⁴² are outstanding in this respect. They showed that the measured line width of YIG spheres can be reduced to a fraction of one oersted by successively finer surface polishing as shown in Figure 17. This implies that the surface irregularities caused by large-grit polishes couple the spin wave modes, thereby broadening the resonance line. They provided further confirmation of Clogston's hypothesis by doing a similar resonance experiment on a thin disk magnetized perpendicular to the plane and found no surface polish effect. Since this latter configuration corresponds to the

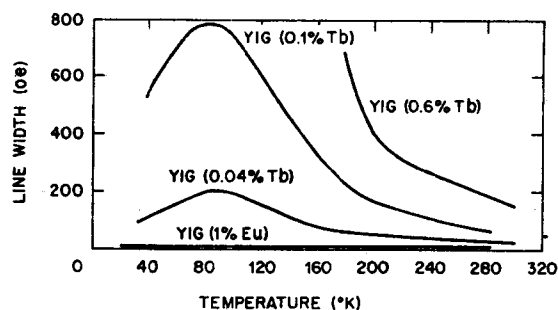


Figure 18—Line width of yttrium-iron garnet at 24 kmc as a function of temperature. Small concentrations of terbium introduce large line-broadening effects. (After Dillon and Nielsen).

lowest allowed frequency on the axis of Figure 14 ($N_T=0$ for the disk), there are few spin waves having the same frequency as the uniform precessional mode.

Role of Impurities.

The effect of impurities on resonance line width in YIG was demonstrated by Dillon and Nielson⁴³ (Figure 18) and by Spencer, LeCraw and Clogston⁴⁰ in their investigation of the resonance properties as a function of temperature. The large line width, with a peak at low temperatures, had been regarded as typical of some ferrimagnets until it was shown to be caused by certain impurities^{43,40} present in very small quantities. Not only has extensive line broadening been observed but also anomalous magnetic anisotropy and modification of the g-factor, in some cases. The physical phenomena involved have now been explained theoretically by Kittel.⁴⁴ In particular, at room temperature and above, the rapid relaxation of the rare earth impurities as compared to the magnetic ions in the normal sublattices determines the g-factor and is responsible for the large line width observed in some of these materials. The very pure yttrium iron garnet that has been developed as a consequence of this research provides an ideal medium for extending the basic studies of relaxation phenomena in ferromagnetic materials. Using such ultra-pure specimens of YIG, Spencer and LeCraw have measured the spin-lattice* relaxation time.^{42,45} They have also made measurements⁴¹ under conditions of high-power saturation and used the relation $h_{crit} = \Delta H (\Delta H_k / 4\pi M)^{1/2}$ to determine ΔH_k , the spin wave line width, as shown in Figure 19. Combining these results with their measurements of the total resonance line width as a function of surface roughness, Fletcher, LeCraw and Spencer⁴⁶ have described the nature of the relaxation process, shown in Figure 20. They have shown that energy is transferred from the mode of uniform precession of the spin dipoles not only directly to the lattice but also via the spin wave modes which subsequently transfer the energy to the lattice. Their latest experimental results have also been interpreted by Sparks and Kittel⁴⁷ who have described and calculated the detailed physical interaction between the spin and the lattice.

V. NONLINEAR PROPERTIES OF FERRITES

The magnetic properties of ferrites are not linearly dependent on the rf field intensity at high signal power. This nonlinear behavior was first demonstrated in cavities in a series of resonance experiments at high microwave power by Bloembergen and Damon, by Damon⁴⁸ and by Bloembergen and Wang.⁴⁹ Some related effects in both cylindrical and rectangular waveguide were reported by Saliotis, Chait and Kales.⁵⁰ The nonlinear properties were first put to use through the invention of the ferrite frequency doubler by Ayres, Vartanian and Melchor.⁵¹ The most significant advance in the understanding of this phenomenon in ferrites was provided by the theoretical work of Anderson and Suhl²⁵ which was developed in detail by Suhl^{25,52} who not only furnished an explanation of the high-power resonance effects that had been observed but also related the phenomena to the spin waves excited in these materials. Suhl

* The spin-lattice relaxation time is the time, on the average, during which a precessing spin dipole loses energy to the lattice and spirals in toward its equilibrium position in alignment with the dc magnetic field.

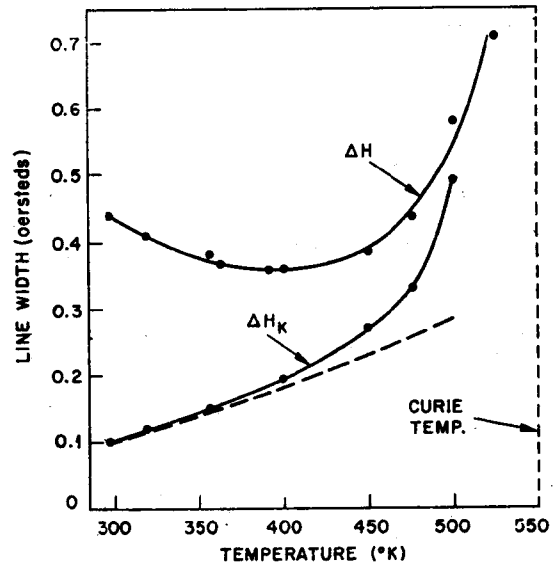


Figure 19 — The line width of the uniform precession (ΔH) and spin waves (ΔH_k) as a function of temperature for YIG at 3330 mc. (After LeCraw and Spencer).

then proposed⁵³ the use of the nonlinear properties in the construction of a *ferromagnetic amplifier* which was subsequently developed by Weiss.⁵⁴ Pulse amplifier performance has been improved and a CW amplifier has now been developed by Denton.⁵⁵

Harmonic Generation.

Both from an historical and pedagogical point of view, the ferrite frequency doubler provides a simple demonstration of the nature of the nonlinear effects in ferrites under conditions of relatively large rf magnetic field intensity. In the expansion of the equation of motion of the magnetization vector,

$$\frac{d\vec{M}}{dt} = \gamma (\vec{M} \times \vec{H}) \quad (10)$$

products of rf quantities may be neglected in the small signal approximation, but these nonlinear terms must be retained for moderately large signal intensity. The mag-

netic field term, \vec{H} , in Equation 10 consists of a static

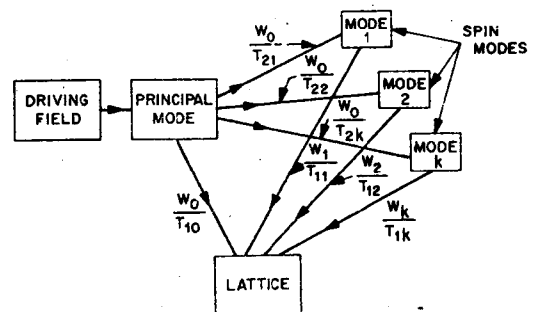


Figure 20 — Schematic diagram of the transfer of energy from the uniform precession of the spins to the lattice both directly and also via the spin wave modes. (After Fletcher, LeCraw and Spencer).

field and a driving field, $\vec{H} = \vec{H}_0 + \vec{h}e^{j\omega t}$ where \vec{h} is smaller than \vec{H}_0 but its magnitude cannot be neglected at high signal levels. The magnetization, \vec{M} , can be expanded

$$\vec{M} = \vec{M}_0 + \vec{m}_1 e^{j\omega t} + \vec{m}_2 e^{2j\omega t} + \dots \quad (11)$$

Assuming \vec{M}_0 and \vec{H}_0 , the static components, to be along the z-direction, and the rf components, particularly \vec{h} , to be arbitrarily disposed, then it can be shown that there is an rf z-component of the magnetization

$$(m_z)_s = \gamma(m_x h_y - m_y h_x) \quad (12)$$

composed of the products of the first-order components of \vec{m} and \vec{h} . This shows that the nonlinear product of these two first-order components gives rise to a harmonic component of the magnetization provided that the rf field within the ferrite specimen is not circularly polarized. In fact, if either h_x or h_y is zero, the harmonic component is a maximum. This is then the nutational component of the gyration at twice the frequency of the driving field. The amplitude of the harmonic component $(m_z)_s$ can be calculated from Equation 10 when the resonance loss mechanism is included. Stern and Pershan⁵⁶ have shown that the amplitude should be inversely proportional to the resonance line width and directly proportional to both the saturation magnetization and the square of the microwave signal intensity. The solution has the form⁵⁷

$$(m_z)_s \approx \omega_M h_x^2 / 4\omega(\Delta H) \quad (13)$$

where $\omega_M = \gamma 4\pi M$, ω is the fundamental frequency, h_x is the input magnetic field intensity and ΔH is the resonance line width. Experiments in the range from 3 kmc to 140 kmc⁵⁸ have verified the relation of Equation 13.

Harmonic generators in rectangular waveguide usually employ a ferrite at the side wall or at the center where the rf driving field is nearly linearly polarized. Conversion efficiencies of 3.5 db have been obtained in the X-band region. In the millimeter wave region, peak power output of 50 watts in the second harmonic has been achieved at 140 kmc. Figure 21 shows the relative output vs input power for ferrimic G and yttrium-iron garnet,⁵⁷ which shows a greater efficiency as the input power is increased. The higher efficiency of YIG is due to its narrower line width.

Saturation Effects.

The early ferromagnetic resonance experiments under conditions of high signal power clearly showed saturation effects in which the susceptibility at resonance declined with increasing power. Classical resonance theory was used initially^{48,49} to explain the dependence of susceptibility on applied power according to the expression⁵⁰

$$\frac{x''(h)}{x''(0)} = \frac{1}{1 + \frac{1}{4} \gamma^2 h^2 T_1 T_2} \quad (14)$$

where $x''(0)$ is the small signal susceptibility and T_1 is

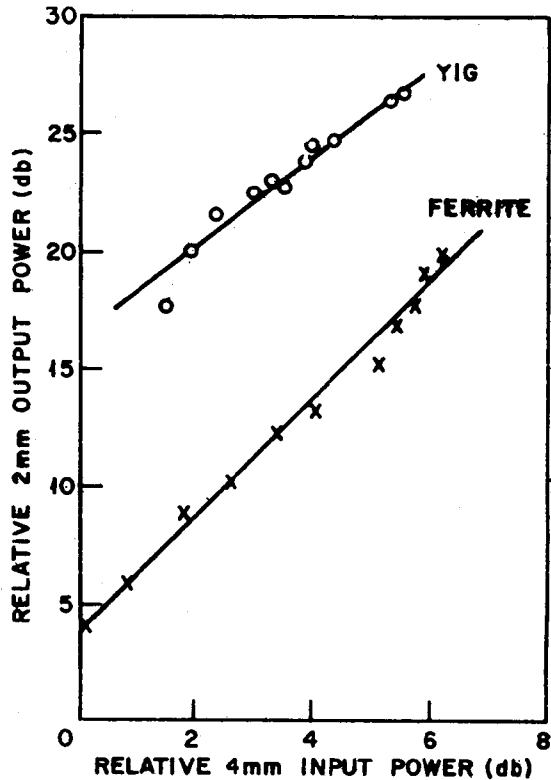


Figure 21 — Input-output curve for frequency-doubling experiment plotted on db scale with arbitrary reference levels. (After Roberts, Ayres and Vartanian).

the spin-lattice relaxation time, defined previously. The phenomenological relaxation time $T = 2/\gamma\Delta H$ is normally used for T_2 . Although this accounted for some of the features of the saturation effects there remained two features which were not fully understood: (1) an abrupt decline in magnetic susceptibility on resonance above a characteristic threshold power level; (2) the growth of a subsidiary "resonance peak" at a field lower than that required for ferromagnetic resonance.

Instability Threshold. The basic concepts of the nonlinear behavior were most clearly developed by Suhl^{59,60} in his explanation of this seemingly anomalous resonance and abrupt decline in susceptibility at the resonance frequency in ferrites at high microwave power levels. The problem was not just that of solving Equation 10 for large signals by retaining second-order terms as in the case of harmonic generation. Actually, it was necessary to explain why the anomalous effects set in at signal levels as much as a hundred times smaller than large signal theory would predict. This led to the derivation, by Anderson and Suhl⁶¹, of an instability or "run-away" condition of m_z , the rf component of the magnetization in the z-direction. In the case of a thin slab magnetized normally and excited by a transverse, circularly polarized rf field, the Kittel resonance frequency is $\omega_r = \gamma(H_0 - 4\pi M_s) = \omega_0 - \omega_{Ms}$ and the rf susceptibility is $x_1 = \omega_{Ms} / (\omega_r - \omega + j/T)$ where $\omega_0 = \gamma H_0$, T is a phenomenological relaxation time, $\omega_{Ms} = (\omega_M^2 - \omega_{Mt}^2)^{1/2}$, $\omega_M = \gamma 4\pi M$ and $\omega_{Mt} = x_1(\gamma h_t)$. This leads to the solution for ω_{Mt}

$\Delta H \sim \Delta H_k$	Critical Field, h_{crit}	
	Theory	Experiment
51	8	9
46	7	5.5
36	5	4
23	2.5	1
7	0.45	0.55

Table I—Suhl's Comparison of Equation 12 with the Experimental Results of Bloembergen and Wang.

$$\omega_{Ms} = \omega_M \left\{ 1 - \frac{1/2 (\gamma h)^2}{[\omega - (\omega_0 - \omega_{Ms})]^2 + \frac{1}{T^2}} \right\} \quad (15)$$

from which we can see, by inspection, the nature of the instability. It is the appearance of ω_{Ms} in the resonance denominator that is of importance. A small disturbance in the uniform precession which may cause the precession angle to increase slightly reduces the component m_x . If, for example, the dc magnetic field has been adjusted to a value somewhat below resonance, this reduction in ω_{Ms} in the resonance denominator brings the denominator closer to its minimum value reducing the value of ω_{Ms} of Equation 15. If this resulting reduction in m_x is larger than the initial slight reduction in m_z , a run-away condition or instability sets in until a new steady-state condition is achieved. The condition for instability can be derived by differentiating the right hand side of Equation 15 with respect to M_x , from which Suhl obtains²⁵

$$h_{crit} = \Delta H \sqrt{\frac{3.08 \Delta H}{4\pi M}} \quad (16)$$

The role of spin waves must also be taken into account in computing the critical field intensity, h_{crit} , for the onset of saturation of the spin system. We are concerned with the mechanism by which energy can be transferred from the uniform precessional mode into spin wave modes of the same frequency and subsequent transfer of energy to the lattice. This modifies the expression of Equation 16 and leads to a somewhat smaller critical field²⁶

$$h_{crit} = \Delta H \sqrt{\frac{2\Delta H_k}{4\pi M}} \quad (17)$$

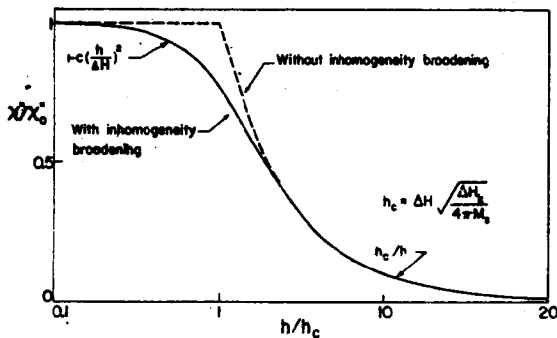


Figure 22—Theoretical dependence of the dissipative part of the susceptibility at ferromagnetic resonance on the rf signal intensity. The dashed line illustrates the instability threshold at h_c described by Suhl. The initial decline in the solid line is attributed to the excitation of spin waves at an inhomogeneity in the specimen. (After Schlömann, Saunders and Sirvetz).

where ΔH_k is the line width of the spin wave resonance. Even for a good single crystal, $\Delta H_k < \Delta H$ in magnitude as shown in Figure 19, but for a polycrystalline specimen, ΔH is liable to be much larger than the intrinsic line width because of broadening of the main resonance line by anisotropy, stresses and porosity. Thus, saturation of the main resonance is reached at h_{crit} where the uniform precessional angle can no longer be increased by increased driving field intensity because of the loss of energy by the spin system to the lattice, both directly and through the spin waves. Suhl has compared his theoretical results with the early experiments and satisfactory agreement is shown in Table I.

Initial Decline of Susceptibility. Suhl's theory accounted for the abrupt decline in susceptibility at resonance observed in ferrites as shown by the dashed line in Figure 22. More recent theoretical work by Schlömann²⁰, Suhl⁶¹ and Seiden⁶² have led to refinements based on the suggestion by Schlömann that imperfections or inhomogeneities in the crystalline lattice of the specimen can "scatter" the uniform precession into spin waves even at very low rf field intensities, well below the instability threshold, h . In that case, an initial decline in susceptibility on resonance should occur as the field intensity is increased as shown by the solid line in Figure 22. Schlömann⁶³, Seiden⁶² and Weiss⁶⁴ have shown experimentally that this is true of imperfect crystals as shown in Figure 23. Thus the transfer of energy to the spin waves increases slowly (except in a perfect crystal) until the catastrophic instability sets in. The expansion of Equation 14 for small values of b yields the form of the decline.

$$\frac{\chi''}{\chi_0} = 1 - C \left(\frac{h}{\Delta H} \right)^2 \quad (18)$$

shown by the initial portion of the solid line in Figure 22. Schlömann has proved, however, that the constant C cannot be interpreted with the phenomenological theory and both Schlömann and Seiden have given an analysis in terms of spin wave interaction terms.

Ferromagnetic Amplifier.

In the discussion of the frequency doubler, the nonlinear terms in the equation of motion of a

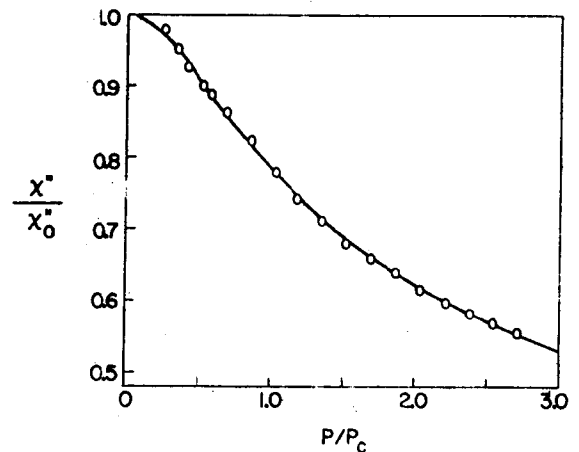


Figure 23—Experimental dependence of susceptibility at resonance on the rf power level in a ferrite ($Mn_{1.4}Fe_{1.6}O_4$) showing an initial decline due to inhomogeneities. (After Weiss).